THE JOURNAL OF PHYSICAL CHEMISTRY B

Article

pubs.acs.org/JPCB

Polarity Controlled Reaction Path and Kinetics of Thermal Cis-to-Trans Isomerization of 4-Aminoazobenzene

Neeraj Kumar Joshi,[†] Masanori Fuyuki,[‡] and Akihide Wada*[,†]

[†]Molecular Photoscience Research Center, Kobe University, 1-1 Rokkodai, Nada, Kobe 657-8501, Japan

[‡]Organization of Advanced Science and Technology, Kobe University, 1-1 Rokkodai, Nada, Kobe 657-8501, Japan

ABSTRACT: Spectral and kinetic behavior of thermal cis-to-trans isomerization of 4-aminoazobenzene (AAB) is examined in various solvents of different polarities. In contrast to azobenzene (AB), it is found the rate of thermal isomerization of AAB is highly dependent on solvent polarity. Accelerated rates are observed in polar solvents as compared to nonpolar solvents. Moreover, a decrease in the barrier height with an increase in medium polarity is observed. Our observations suggest that inversion is the preferred pathway in cis-to-trans thermal isomerization in a nonpolar medium; however, in a polar medium, the isomerization path deviates from the inversion route and rotational behavior is incorporated. Differences in the kinetics and in mechanisms of isomerization in different media are rationalized in terms of modulation in barrier height by polarity of the medium and solute−solvent interaction. It is found that kinetics as well as the mechanism of thermal isomerization in AAB is controlled by the polarity of the medium.

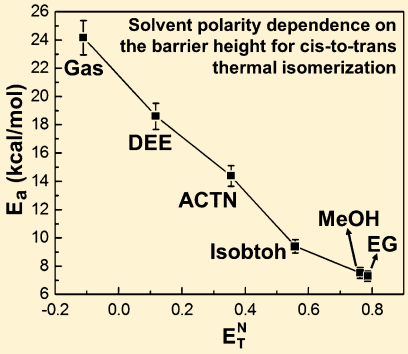

1. INTRODUCTION

Photoinduced studies provide information regarding various radiative and nonradiative relaxation processes by which an excited molecule returns to its ground state. The family of azobenzene derivatives (ABD) is photolabile, and photoinduced modifications in their case have long been known.[1−41] ABD can exist either in cis or trans conformations. The cis form is energetically less stable as compared to the trans form. Trans → cis photoisomerization occurs following irradiation with UV−visible light. On the other hand, cis → trans thermal isomerization occurs spontaneously in the dark owing to the thermodynamic stability of the trans isomer. In addition to thermal isomerization, photoinduced cis → trans isomerization is also possible. Such easy interconversion between the two isomers makes ABD a widely used organic chromophore for technical applications, including optical waveguides and shutters,[1] switching display devices,[2,3] optical memories,[4,5] electro-optical modulators,[6] photoactive artificial muscles,[7−9] light-triggered nanomachines,[10,11] etc.

Azobenzene (AB) has been a subject of interest and investigation on the mechanism of isomerization process (either photoinduced or thermal).[11−21] X-ray and computational data indicate *trans*-AB adopts a planar structure with C_{2h} symmetry,[22,23] while *cis*-AB possesses a nonplanar conformation with C_2 symmetry.[24,25] The absorption spectrum of *trans*-AB consists of two well separated bands in the UV−visible region.[26,27] The strong UV band (320 nm) arises from the symmetry allowed $\pi \rightarrow \pi^*$ (S_2 - second excited singlet) transition.[11,28] The much weaker band in the visible region (450 nm) corresponds to the symmetry forbidden $n \rightarrow \pi^*$ (S_1 - first excited singlet) transition.[11] The $\pi \rightarrow \pi^*$ transition of *cis*-AB (260 nm) is weaker, but the $n \rightarrow \pi^*$ transition (440 nm) absorbs more strongly than *trans*-AB.[14]

Furthermore, trans ↔ cis interconversion can be controlled by irradiating either transitions[11] and/or by changing the intensity of irradiating monochromatic radiation.[28,29] In general, for photoisomerization of AB, four possible mechanisms have been proposed, i.e., rotation, inversion, concerted inversion, and inversion assisted rotation.[11,23,30,31] The transition state formed in concerted inversion has no net dipole moment, whereas the other three pathways possess polar transition states.[21] Relaxation from all four transition states can afford either the cis or trans isomer; therefore, all four mechanisms predict photostationary states consisting of both isomers.[21] It has been shown theoretically[23,32−36] and experimentally[37−41] that the thermal cis → trans isomerization of AB proceeds via an inversion mechanism. Theoretical calculations predict a significantly larger activation energy for rotation (36.2 kcal/mol) as compared to inversion (24.9 kcal/mol).[23] The rate of thermal isomerization is also found independent of solvent polarity, which is also indicative of inversion as the preferred pathway.[21]

Substitution by different groups at different positions in the parent moiety (AB) can alter spectroscopic properties and dynamics/kinetics of isomerization.[36−40] On substituted AB, solvents also greatly influence the photostationary state and rate of thermal isomerization reaction.[12,36,41−44] Substitution of an amino group ($-NH_2$) at the 4-position in *trans*-AB, i.e., *trans*-4-aminoazobenzene (*trans*-AAB), shifts the $\pi \rightarrow \pi^*$ absorption

Received: December 20, 2013
Revised: January 24, 2014
Published: January 26, 2014

   dx.doi.org/10.1021/jp4125205 | *J. Phys. Chem. B* 2014, 118, 1891−1899

band (compared to *trans*-AB) toward longer wavelength, causing an overlap with the n → π* absorption band.[40] In contrast to *trans*-AB, n → π* absorption is buried under the intense π → π* absorption band of *trans*-AAB. An energy gap (difference between π → π* and n → π* states) of 3000−4000 cm^{-1} was estimated for *trans*-AAB in ethanol,[40] which is smaller than the energy gap of *trans*-AB (~10 000 cm^{-1}). The photoisomerization dynamics of the π → π* excited *trans*-AAB in ethanol and heptanol were investigated by using UV−vis transient absorption spectroscopy by Hirose et al.[40] The transient absorption spectra of the π → π* excited *trans*-AAB showed that the internal conversion process from the n→ π* state to the ground state corresponded well to that of the *trans*-AB directly excited to the n→ π* state, not to that of the π → π* excited *trans*-AB. This result indicates that the photoisomerization of π → π* excited *trans*-AAB proceeded with different pathways from the π → π* excited *trans*-AB. Study by Hirose et al.[40] suggests that spectral features as well as dynamics of photoisomerization of *trans*-AAB are quite different from its parent *trans*-AB.

Photoinduced trans-to-cis (forward), photoinduced cis-to-trans (reverse), and thermal cis-to-trans isomerization (back) reactions are the major relaxation processes in the photoreaction network (Figure 1) of the ABD system. The forward

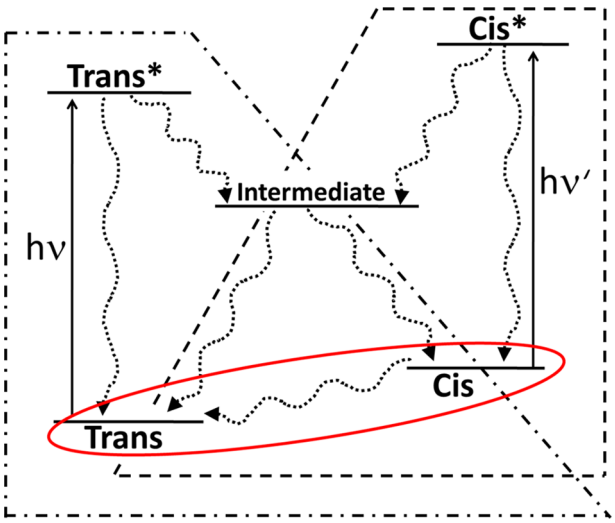

Figure 1. Schematic diagram of the photoreaction network of azobenzene derivatives. Details are given in the text.

(covered by a dash-dotted line in Figure 1) and reverse reaction (covered by only a dashed line in Figure 1) can coexist depending on the choice of excitation wavelength and generally occurs in an extremely short time scale (fs to sub-ps regime). However, once a cis form is generated, it thermally relaxes (in dark) to its stable trans ground state configuration. For realization of complete tale of such complex photoreaction network, detailed knowledge about all deactivation processes of the photonetwork is quite helpful. The knowledge of the back reaction (highlighted by a red line in Figure 1), one of the important reactions in a network, can help in understanding and control of the whole photoreaction network.

As discussed earlier, the photoinduced dynamics (forward reaction) of AAB is quite different from its parent AB,[40] so it is also interesting to investigate the back reaction in AAB. Although based on the theoretical calculations,[32,43,44] few reports on thermal cis-to-trans isomerization of AAB are available which do not encompass the solvent polarity and viscosity effect in detail. In this paper, to decipher the mechanism of isomerization in the ground state and to obtain details about one of the deactivation processes of a photoreaction cycle, we focus our study on the kinetics of thermal isomerization of 4-aminoazobenzene (AAB) under the dependence of solvent polarity, viscosity, and temperature. To the best of our knowledge, thermal cis-to-trans isomerization of AAB has not been systematically investigated experimentally yet. Therefore, systematic experiments are performed to obtain better insight on the thermal cis-to-trans isomerization of AAB.

2. EXPERIMENTAL SECTION

2.1. Materials. 4-Aminoazobeneze (AAB) obtained from Wako Pure Chemical Industries, Ltd., Japan (99% pure), was used as such. All the solvents used were of spectroscopic grades. The polarity parameter and viscosity of the solvents are listed in Table 1.

Table 1. Estimated Value of the cis Population in the Photostationary State in Different Media

medium	E_T^N [a]	η [b] (cP)	cis population (%)
DEE	0.117	0.224	91.6
ACTN	0.355	0.306	88.4
IBOH	0.552	3.95	66.8
MEOH	0.762	0.544	34.3
EG	0.781	16.1	11.7

[a]Reference 50. [b]Reference 56, temperature at 298 K.

2.2. Instrumentation. Steady state absorption spectra were recorded by a dual beam Shimadzu UV-2400PC spectrophotometer. For temperature dependent measurements, a facility (Circulating Bath/Immersion Circulator, Polyscience, USA) is available with the sample compartment. The temperature measurement has an accuracy of ±1 °C. To generate *cis*-AAB, a cw UV laser (405 nm, ~200 mW, purchased from World Co. Ltd., Japan) was used. The power of the laser source was measured through a Gentec TPM 300 power meter. Time resolved measurements for a time constant longer than 1.0 s were carried out by sequential accumulation of the spectrophotometer. To measure the temporal behavior with a time constant shorter than 1.0 s, a time-resolved setup was built (shown in Figure 2). In the setup, a pump UV laser beam was modulated by a mechanical chopper and the transient absorption changes were monitored by a probe beam. An electric lamp (MINI MAGLITE 2AA) was used as the source for the probe beam. Pump and probe beams were focused and

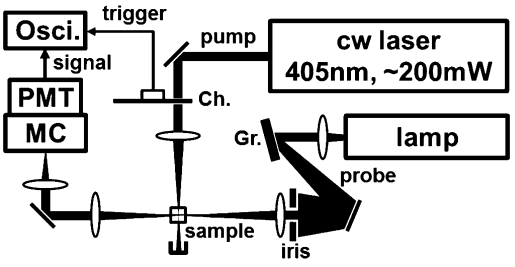

Figure 2. Schematic diagram of the home-built setup to observe temporal absorbance change at a time constant shorter than 1.0 s. Ch, mechanical chopper; Gr, grating; MC, monochromator; Osci, oscilloscope; PMT, photomultiplier tube.

dx.doi.org/10.1021/jp4125205 | J. Phys. Chem. B 2014, 118, 1891−1899

overlapped in the quartz cell of 2 mm path length. The intensity of the transmitted probe beam was detected by a PMT (R928, Hamamatsu) coupled with a monochromator (JASCO, CT10). Temporal behavior of the intensity was observed and accumulated by a digital oscilloscope (Tektronix, 200 MHz, 2GS/s) which was synchronized to on/off modulation of the pump beam. In all solvents, the concentration of the AAB was approximately 4×10^{-5} M. To prevent photoisomerization caused by any other radiation, e.g., room light, all experiments were carried out in the dark room.

2.3. Calculation Details. Calculations were performed using the Gaussian 03 package.[45] The trans and cis isomers for the thermal isomerization of 4-AAB in the ground state were optimized unrestrainedly by means of the DFT methods. The 6-31G* basis set was used in the B3LYP calculations. In order to locate and optimize the transition state (TS) structure in the gas phase, the synchronous transit-guided quasi-Newton (STQN) method[46,47] with QST2 option was employed at the DFT-B3LYP/6-31G* level. All optimized structures (cis isomer, trans isomer, and TS structure) were confirmed by vibrational frequency analysis. Only real frequency values were obtained for the cis and trans isomer, and a single imaginary frequency was shown by TS structure. Calculations in solvents were performed employing the self-consistent reaction field (SCRF) method based on the polarizable continuum model (PCM).[48,49]

3. RESULTS AND DISCUSSION

3.1. Effect of Solvent and Temperature on Thermal Isomerization. Absorption spectra of AAB are recorded in solvents of different polarities, viz, diethyl ether (DEE), acetone (ACTN), isobutanol (IBOH), methanol (MEOH), and ethylene glycol (EG). The polarity of the solvent is defined by the dimensionless microscopic solvent polarity parameter E_T^N proposed by Reichardt.[50]

Absorption spectra (at 298 K) of AAB in DEE (E_T^N = 0.117) and MEOH (E_T^N = 0.762) are shown in Figures 3a and 4a,

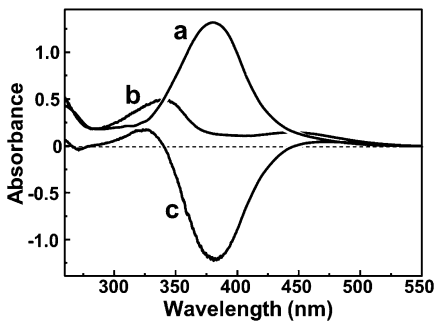

Figure 3. Absorption spectra of AAB in DEE: (a) absorption spectrum before UV irradiation; (b) absorption spectrum under UV irradiation (photostationary state); (c) difference spectrum between spectrum a and spectrum b.

respectively. AAB exhibits an absorption maximum at ~380 nm with a long wavelength absorption tail. In all studied solvents, no significant effect of polarity on the absorption maximum is observed for AAB. The absorption maximum of AAB is also found to be independent of the solute concentration, and hence, the possibility of solute aggregation is ruled out in all studied solvents. As discussed,[40] the absorption band at ~380 nm is attributed to $\pi \rightarrow \pi^*$ transition of *trans*-AAB, while the

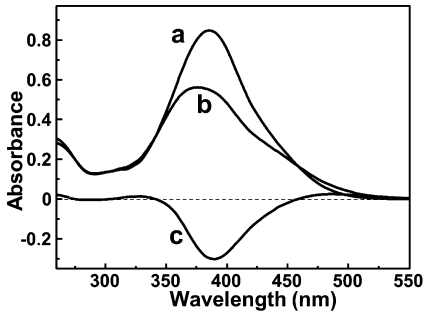

Figure 4. Absorption spectra of AAB in MEOH: (a) absorption spectrum before UV irradiation; (b) absorption spectrum under UV irradiation (photostationary state); (c) difference spectrum between spectrum a and spectrum b.

absorption band corresponding to n $\rightarrow \pi^*$ transition of *trans*-AAB is so weak that it is buried under the $\pi \rightarrow \pi^*$ transition and appears as a long wavelength tail.

To generate *cis*-AAB, the UV laser (405 nm) was irradiated (approximately for 10−15 s) until it reached a photostationary state (Figures 3b and 4b). The absorption profile of the photostationary state is recorded under the irradiation of an UV laser (405 nm). In DEE, under the irradiation of an UV laser (photostationary state), a large decrease in absorbance at around 380 nm with two newly developed absorption bands at around 330 nm and around 455 nm is observed (Figure 3b). However, in MEOH (Figure 4b), the profile of the photostationary state is entirely different from that of DEE. Subsequently, we observe that the profile of the photostationary state and decrease in the absorbance strongly depends on the polarity of the medium (discussed in detail later).

In the case of DEE, in the photostationary state (Figure 3b), the broad absorption profile with two well separated bands indicates the presence of *cis*-AAB. In the difference spectrum (Figure 3c), negative absorbance at ~380 nm is assigned to the photobleaching of *trans*-AAB and the absorption peaks at around 330 nm and around 465 nm are attributed to *cis*-AAB. In analogy with AB (the energy gap between $\pi \rightarrow \pi^*$ and n $\rightarrow \pi^*$ transition is larger for *cis*-AB than *trans*-AB, and the $\pi \rightarrow \pi^*$ band shows blue shift and weakening[11,14,28]), the short wavelength absorption band (330 nm) is assigned as the $\pi \rightarrow \pi^*$ transition of *cis*-AAB, while the long wavelength absorption band (465 nm) is attributed to the n $\rightarrow \pi^*$ transition of *cis*-AAB. Here, we would like to mention that, in DEE, the energy gap (in the $\pi \rightarrow \pi^*$ and n $\rightarrow \pi^*$ states) of *cis*-AAB is ~8800 cm^{-1}, which is much larger than the energy gap for *trans*-AAB (~3000−4000 cm^{-1}). On the other hand, assignment of the bands of cis form from the profile of the photostationary state in MEOH (Figure 4b) is more complicated than for DEE.

In a particular medium, in the photostationary state, the ratio between the cis to trans form depends on the intensity of the pump light, the rate of thermal isomerization reaction, and the absorption cross section of each isomer. Under the assumption that the peak intensity of the trans form at the absorption maximum wavelength (380 nm) is only due to the trans form (i.e., no cis form is present), the cis isomer present in the photostationary state can be estimated by the decrease in the absorbance at this wavelength. Using the absorption spectrum, the population ratio (PR) of the cis form of AAB in the photostationary state can be estimated from the following formula as

dx.doi.org/10.1021/jp4125205 | J. Phys. Chem. B 2014, 118, 1891−1899

$$\text{population ratio of cis: PR} = \frac{[A_\lambda]_{wi} - [A_\lambda]_{ui}}{[A_\lambda]_{wi}} \times 100 \quad (1)$$

where the subscripts wi and ui refer to without irradiation and under irradiation of UV laser, respectively. A_λ is the absorbance at wavelength λ, where λ is the wavelength of absorption maximum of the trans form. Using eq 1, the effect of polarity and viscosity of the solvent on the estimated population of *cis*-AAB in the photostationary state is shown in Table 1. From Table 1, it can be noticed that, compared to the solvent viscosity, the polarity of the solvent plays a major role on the photostationary state (discussed in detail later). Lesser change in absorption profile, namely, decrease of *cis*-AAB population, in polar medium indicates a lesser thermodynamic stability of *cis*-AAB in the ground state, i.e., the faster ground state isomerization from cis to trans forms as compared to nonpolar medium.

Once the irradiation of the UV laser (405 nm) is stopped, as a matter of fact, the absorption intensity of cis peaks (330 and 465 nm) decreases and simultaneously absorption corresponding to the trans peak begins to increase, as shown in Figure 5.

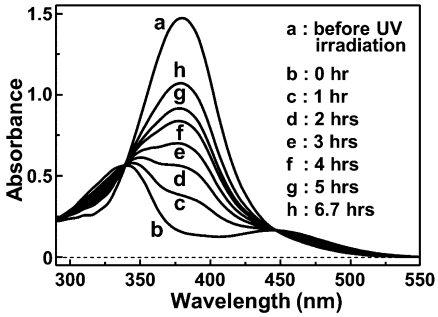

Figure 5. Temporal behavior of the absorption profile of AAB in DEE after UV irradiation, showing the cis-to-trans conversion in the dark at 295 K. Delay times (after stopping the irradiation of the pump beam) of observation are presented in the figure.

Figure 5 exhibits the absorption profiles in DEE monitored at different time intervals after the removal of the UV laser. Temporal profiles of the trans peak intensity at different temperatures are depicted in Figure 6.

Generally, the rate of thermal isomerization reaction follows a first-order kinetics. The unimolecular thermal cis-to-trans isomerization reaction in the dark obeys eq 2

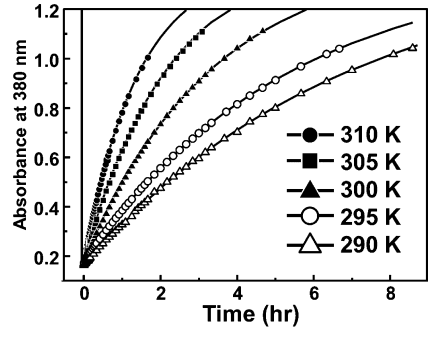

Figure 6. Temporal behavior of absorbance at 380 nm of AAB in DEE after stopping UV irradiation at different temperatures. Solid lines indicate the results of the least-squares fitting of the data to eq 2.

$$A(t) = A_\infty + A_1 \exp\left(-\frac{t}{\tau}\right) \quad (2)$$

where $A(t)$ and A_∞ correspond to the absorbance of AAB at any time t and absorbance as time approaches infinity, respectively. A_1 is the pre-exponential factor, and τ is the lifetime of the ground state of *cis*-AAB. The lifetimes were recovered from the plots by the least-squares fitting of the data to eq 2. Lifetimes were determined with an associated error lower than 5% in all cases.

The effect of temperature on the rate of thermal isomerization reaction was also investigated. Lifetimes (τ) and reaction rate ($k = 1/\tau$) in different media at different temperatures are summarized in Table 2. It is indicated from

Table 2. Temperature Dependent Lifetime and Rate of Thermal Isomerization Reaction

solvent (E_T^N)	temperature (K)	τ (s)	$k_{c\to t}$ (s^{-1})
DEE (0.117)	290	2.61×10^4	3.82×10^{-5}
	295	2.02×10^4	4.95×10^{-5}
	300	1.13×10^4	8.84×10^{-5}
	305	6.55×10^3	15.25×10^{-5}
	310	3.38×10^3	29.55×10^{-5}
ACTN (0.355)	290	2.46×10^4	4.10×10^{-5}
	295	1.92×10^4	5.20×10^{-5}
	300	1.18×10^4	8.42×10^{-5}
	305	7.93×10^3	12.60×10^{-5}
	310	5.11×10^3	19.56×10^{-5}
IBOH (0.554)	290	1.47×10^2	6.82×10^{-3}
	295	1.22×10^2	8.21×10^{-3}
	300	93.1	10.74×10^{-3}
	305	73.4	13.62×10^{-3}
	310	52.4	19.07×10^{-3}
MEOH (0.762)	278	1.05	0.94
	283	0.90	1.11
	288	0.70	1.42
	293	0.58	1.72
	298	0.42	2.38
EG (0.781)	280	0.26	3.85
	285	0.22	4.55
	290	0.19	5.26
	295	0.13	7.70

Table 2 that the lifetime of the ground state of the cis form strongly depends on the polarity of the medium. In DEE, the estimated lifetime at 300 K is approximately 1.13×10^4 s (~188 min), while it comes out to be 0.42 s in MEOH. The data in Table 2 clearly shows accelerated rates in polar media, and illustrates that in a particular medium reaction is temperature dependent; on lowering the temperature, the reaction becomes slower.

Further, the rate of reaction is governed by barrier height and it can be estimated using temperature dependent reaction rates and employing the Arrhenius equation as follows

$$k_{c\to t} = A \exp\left(-\frac{E_a}{RT}\right) \quad (3)$$

where $k_{c\to t}$ is the rate constant of thermal isomerization reaction from cis to trans, T is the absolute temperature, R is the universal gas constant, and A is the pre-exponential factor (frequency factor). The term E_a is used for the barrier height in the Arrhenius equation. Arrhenius plots for different solvents

dx.doi.org/10.1021/jp4125205 | J. Phys. Chem. B 2014, 118, 1891−1899

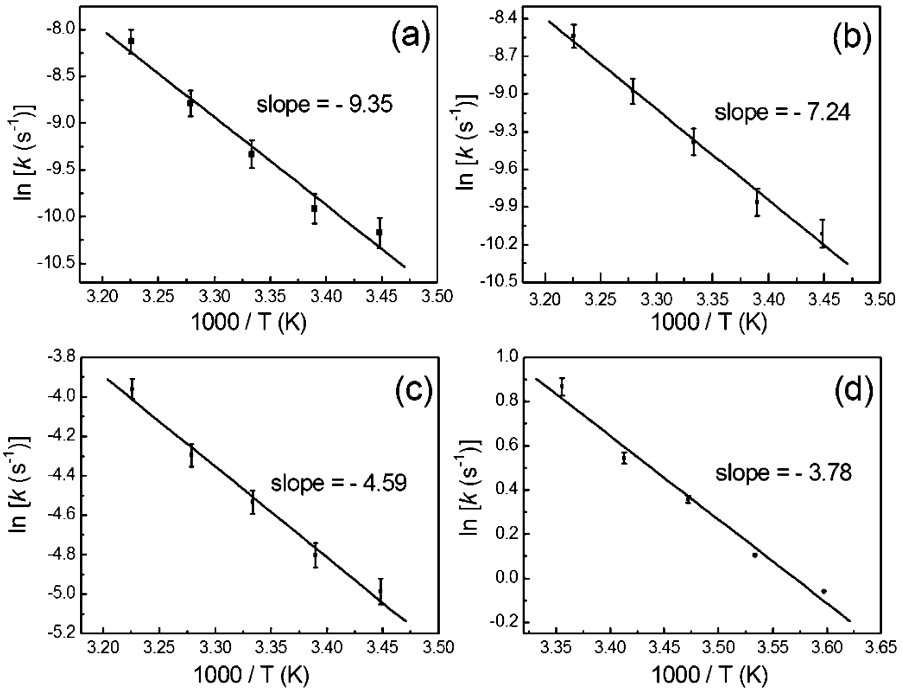

Figure 7. Arrhenius plot in different solvents: (a) DEE, (b) ACTN, (c) IBOH, and (d) MEOH.

are shown in Figure.7. The solid straight lines in the Arrhenius plot represent the linear fitting of the data, and the slope of these lines is used to estimate the barrier height (E_a). We have also theoretically calculated the barrier height in the gas phase (using the STQN method), which is 24.2 (±1.2) kcal/mol. The plot between solvent polarity and barrier height is shown in Figure 8 which shows the polarity dependence of the obtained

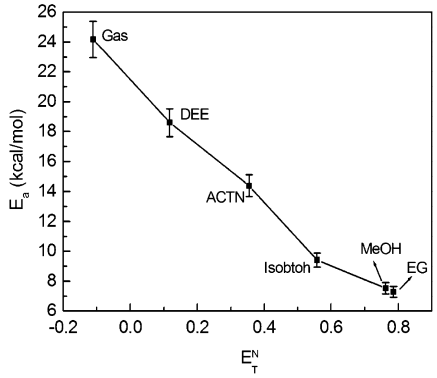

Figure 8. Barrier height and solvent polarity parameter. The error in the barrier height for gas is assumed similar to that observed in the experimental value for solvents. 1 kcal/mol = 4.18 kJ/mol.

barrier height. It is shown from the figure that the barrier height almost linearly decreases with an increase in polarity of the solvent. The decrease in the value of E_a is in the following order: 24.2 (±1.2) kcal/mol (gas) >18.5 (±0.9) kcal/mol (DEE) > 13.8 (±0.7) kcal/mol (ACTN) > 9.1 (±0.5) kcal/mol (IBOH) > 7.5 (±0.4) kcal/mol (MEOH). Using the quantum chemical approach, Dokic et al.[32] calculated E_a as approximately 25.1 kcal/mol for AAB in the gas phase.

We have also examined the effect of viscosity on the reaction rate of thermal isomerization. For this purpose, ethylene glycol (EG) was chosen, as its viscosity is much higher (16.1 cP at 298 K) as compared to the MEOH (0.55 cP at 298 K); on the other hand, the E_T^N value of EG (E_T^N = 0.781) is similar to that of MEOH (E_T^N = 0.762). It should be mentioned that, upon UV laser (405 nm) irradiation in EG, the change in absorption spectrum (Figure 9) was lesser as compared to MEOH. In EG,

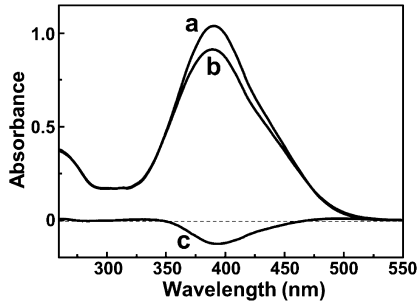

Figure 9. Absorption spectrum of AAB in EG: (a) absorption spectrum before UV irradiation; (b) absorption spectrum under UV irradiation (photostationary state); (c) difference spectrum between spectrum a and spectrum b.

the estimated cis population of AAB in the photostationary state is ~11.7% (Table 1). Additionally, due to the high viscosity of EG, one may expect a longer lifetime of the ground state of *cis*-AAB. On the contrary, faster kinetics is observed in EG as compared to MEOH (Table 2). Apparently, viscosity does not slow the thermal reaction rate. This result is in good agreement with the other reports for similar types of molecules.[20,51] From temperature dependent ground state decay behavior of *cis*-AAB in EG, the estimated barrier height comes out to be 7.3 (±0.4) kcal/mol which is slightly less than that in MEOH probably due to the slightly higher value of E_T^N of EG as compared to MEOH. This result also indicates that, in a particular solvent, a decrease in reaction rate on lowering the temperature is not due to increased viscosity of the solvent. Therefore, the barrier height for thermal cis-to-trans isomer-

dx.doi.org/10.1021/jp4125205 | J. Phys. Chem. B 2014, 118, 1891−1899

ization in AAB can be correlated to the solvent polarity parameter (E_T^N) of the surrounding medium. In the foregoing discussion, we see the decrease in the barrier height with an increase in the polarity of the medium (Figure 8); thus, higher rates are noticed in higher polar medium. Following our results, it appears that increased polarity of the medium may affect the reaction in three possible ways: (i) by affecting the energy of the transition state but the relative stability of *cis*-AAB remains unaffected (Figure 10-i), (ii) by affecting the energy of *cis*-AAB

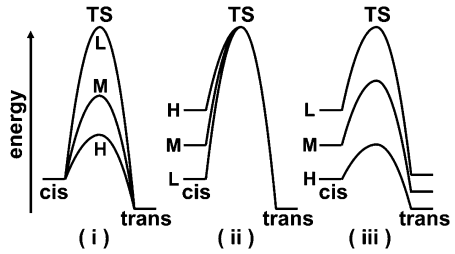

Figure 10. Schematic diagram for various considered models. TS, transition state; H, high polarity; M, medium polarity; L, low polarity.

but the energy of the transition state remains unaltered (Figure 10-ii), and (iii) by affecting simultaneously both the relative stability of *cis*-AAB and the transition state (Figure 10-iii). In all cases, the barrier height will change and reflects in the rate constant of the reaction. In order to verify these proposed models, computational calculations were carried out.

3.2. Relative Stability, Dipole Moments, and Transition State. The optimized structures of *trans*- and *cis*-AAB in the gas phase are shown in Figure 11 and well match with the previous reports.[43] In the gas phase, the ground state dipole moments of the *trans*- and *cis*-AAB are 3.11 and 4.95 D, respectively. Silva et al.[53] have reported the dipole moment value of *trans*-AAB, i.e., 3.05 D (in the gas phase). This value is very similar to that which we obtained (3.11 D). Values of the ground state dipole moments of optimized *trans*- as well as *cis*-AAB in solvents are shown in Table 3. The results of calculations in DEE, ACTN, and MEOH show that the ground state dipole moments of both *trans*- and *cis*-AAB increase with an increase in the polarity of the medium. Further, the ground state energies of the cis form, trans form, and transition state (TS) in the gas phase were obtained using computational calculation through optimization. TS energies in solvents are obtained from the sum of the ground state energy of the cis form (obtained using computational calculation) and the estimated barrier height. The results of calculated and estimated energies of each form in different media are summarized in Figure 12. From Figure 12, it is clear that each form is stabilized with an increase in the polarity of the medium, namely, Figure 10-iii. As listed in Table 3, the dipole moment of the cis and trans form increases with an increase in polarity. Stabilization of

Table 3. Theoretically Estimated Dipole Moments in the Ground State by DFT-B3LYP/6-31G*

medium	μ_{cis} (D)	μ_{trans} (D)
gas	4.95	3.11
DEE	6.36	4.02
ACTN	6.99	4.43
MEOH	7.65	4.49

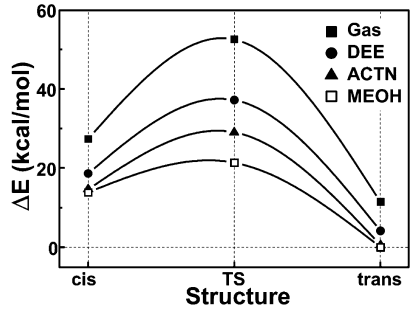

Figure 12. Solvent dependence of the energy of cis, trans, and transition state (TS) of AAB compared to *trans*-AAB in MEOH. Solvents are indicated in the figure. The energy of the transition state structure is estimated by using the experimental value of barrier height except for gas. Solid lines are guide for eyes. 1 kcal/mol = 4.18 kJ/mol.

the cis and trans form is thereby rationalized as the higher dipole moment is stabilized by the polar medium.[23]

In order to analyze the TS character, the energies of different structures are plotted as a function of solvent polarity, as shown in Figure 13. The solid lines indicate the results of linear fitting

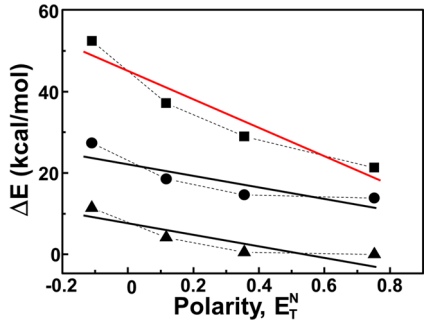

Figure 13. Polarity dependence on energy of TS (■), *cis*-AAB (●), and *trans*-AAB (▲) compared to *trans*-AAB in MEOH. Solid lines are results of linear fitting of the data. The steepness of the slope for TS is emphasized by the red-colored line. Dashed lines are guides for the eyes. 1 kcal/mol = 4.18 kJ/mol.

of the data. It is evident from Figure 13 that the slope of the linear fit for the TS structure is much steeper than the slope of the linear fit for the cis and trans forms, which fairly indicates that with an increase in solvent polarity stabilization of TS is

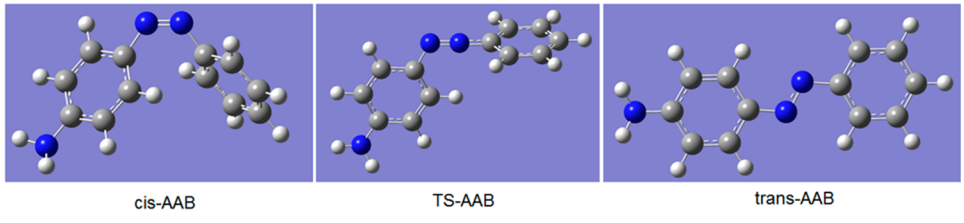

Figure 11. Optimized structures of AAB in the gas phase using DFT-B3LY/6-31G*.

dx.doi.org/10.1021/jp4125205 | J. Phys. Chem. B 2014, 118, 1891−1899

greater than stabilization of the cis and trans forms. From these results, it can be predicted that the TS should possess a higher dipole moment and polar character in polar medium as compared to less polar medium. Although the possibility of a different TS structure in a polar medium as compared to that in a relatively less polar medium cannot be ruled out, it is feasible only if the mechanism of isomerization is different in a polar medium than a nonpolar medium.

Further, the TS structure in the gas phase was searched computationally using the STQN (QST2) method. The optimized TS structure is shown in Figure 11 which corresponds to the inversion mechanism.[43,44,52] With DEE being nonpolar in character, thermal isomerization through inversion can be expected. Faster relaxation times in polar media are evidence that intermolecular interaction between the solute and the solvent molecules can influence the rate of the isomerization process for AAB. In 4-hydroxy azobenzene (HAB), higher rates in polar solvents have also been repoted.[36] In HAB, formation of intermolecular hydrogen bonds favors rotation,[36,54,55] which seems to be the key for the faster isomerization kinetics in polar medium. In analogy to HAB,[36] solute−solvent interaction such as intermolecular hydrogen bonding is also feasible for AAB in polar medium. Therefore, it is worth considering interaction then a polar medium. This results in a higher stabilization of TS and hence lowering in the barrier height, which results in accelerated rates. Additionally, a polar TS with charge separation can lower the activation energy and favor rotation.[35] The formation of a charged TS should be favorable in polar solvents. Therefore, a rotation mechanism which involves a more polar TS than the TS of the inversion mechanism may be involved for thermal *cis*-AAB to *trans*-AAB in solvents of higher polarity.

In comparison to AB, where the reaction path as well as kinetics of thermal cis-to-trans isomerization is independent of polarity,[21] it is found that thermal cis-to-trans isomerization in AAB is highly sensitive toward the polarity of the medium. As it has been observed that substitution of an amino group at the 4-position in AB alters the dynamics of photoisomerization as compared to AB,[40] similarly, results presented here indicate that thermal isomerization is also influenced by substitution of an amino group at the 4-position in AB. It is natural to consider from the results that the polarity and the electron donor character of the substituent play an important role for the onset of the solvent dependency. However, the details on the mechanism of solvent dependency still need to be investigated comprehensively by theoretical calculation.

CONCLUSION

We investigated the kinetics of the thermal isomerization reaction of AAB in solvents of varying polarities. The effect of temperature and viscosity on the isomerization reaction is also investigated. Our investigations reveal some salient features of the isomerization reaction of AAB. The rate of thermal isomerization of AAB is highly dependent on solvent polarity. In contrast to nonpolar solvents, accelerated rates are observed in polar medium. A positive correlation between barrier height and the polarity of the medium is observed. Accelerated rates and stability of various forms in solvents of higher polarity suggest that solute−solvent interaction especially the hydrogen bonding network of solute and solvent can influence the isomerization reaction compared to nonpolar solvents. We have also observed that increased viscosity of the medium does not hinder the thermal isomerization reaction of AAB. Our observations suggest that the mechanism for cis-to-trans thermal isomerization is greatly influenced by the polarity of medium. Our investigation supports a model similar to that as proposed in Figure 10-iii to explain the observed features of thermal isomerization of AAB. In a nonpolar medium, the inversion mechanism seems to be preferred. However, it is believed that the rotation mechanism occurs in a polar medium.

Furthermore, on excitation, either via one photon or multiphoton can have involvement of higher excited states such as S_2 or S_n but the thermal isomerization is the final deactivation process in a photoreaction network of the ABD system. Therefore, these findings on the thermal isomerization are important to the understanding and control of the photoreaction network even in the case of multiphoton excitation.

AUTHOR INFORMATION

Corresponding Author

*E-mail: aki.wada@koala.kobe-u.ac.jp. Phone: +81-78-803-5695.

Notes

The authors declare no competing financial interest.

ACKNOWLEDGMENTS

Prof. Shunji Kasahara, Molecular Photo Science Research Center, Kobe University, Kobe, Japan, is greatly acknowledged for providing us use of their facility of Gaussian 03 software and system. This work was financially supported by a Grant-in-Aid for Challenging Exploratory Research (Grant No. 24655015) from the Japan Society for the Promotion of Science (JSPS).

REFERENCES

(1) Bang, C. U.; Shishido, A.; Ikeada, T. Azobenzene Liquid-Crystalline Polymer for Optical Switching of Grating Waveguide Couplers with a Flat Surface. *Macromol. Rapid Commun.* **2007**, *28*, 1040−1044.

(2) Yager, K. G.; Barrett, C. J. Novel Photo-switching using Azobenzene Functional Materials. *J. Photochem. Photobiol., A* **2006**, *182*, 250−261.

(3) Beharry, A. A.; Sadovski, O.; Woolley, G. A. Azobenzene Photoswitching without Ultraviolet Light. *J. Am. Chem. Soc.* **2011**, *133*, 19684−19687.

(4) Gibbons, W. M.; Shannon, P. J.; Sun, S. T.; Swetlin, B. J. Surface-mediated Alignment of Nematic Liquid Crystals with Polarized Laser Light. *Nature* **1991**, *351*, 49−50.

(5) Ikeda, T.; Tsutsumi, O. Optical Switching and Image Storage by Means of Azobenzene Liquid-Crystal Films. *Science* **1995**, *268*, 1873−1875.

(6) Luk, Y. Y.; Abbott, N. L. Surface-Driven Switching of Liquid Crystals Using Redox-Active Groups on Electrodes. *Science* **2003**, *301*, 623−626.

(7) Camacho-Lopez, M.; Finkelmann, H.; Palffy-Muhoray, P.; Shelley, M. Fast Liquid-Crystal Elastomer Swims into the Dark. *Nat. Mater.* **2004**, *3*, 307−310.

(8) Yamada, M.; Kondo, M.; Mamiya, J. I.; Yu, Y.; Kinoshita, M.; Barrett, C. J.; Ikeda, T. Photomobile Polymer Materials: Towards Light-Driven Plastic Motors. *Angew. Chem., Int. Ed.* **2008**, *47*, 4986−4988.

(9) Yin, R.; Xu, W.; Kondo, M.; Yen, C. C.; Mamiya, J. I.; Ikeda, T.; Yu, Y. Can Sunlight Drive the Photoinduced Bending of Polymer Films? *J. Mater. Chem.* **2009**, *19*, 3141−3143.

(10) Yu, Y. L.; Nakano, M.; Ikeda, T. Photomechanics: Directed Bending of a Polymer Film by Light. *Nature* **2003**, *425*, 145−145.

(11) Rau, H.; Lueddecke, E. On the Rotation-Inversion Controversy on Photoisomerization of Azobenzenes. Experimental Proof of Inversion. *J. Am. Chem. Soc.* **1982**, *104*, 1616−1620.
(12) Asano, T.; Okada, T.; Thermal, Z-E Isomerization of Azobenzenes. The Pressure, Solvent, and Substituent Effects. *J. Org. Chem.* **1984**, *49*, 4387−4391.
(13) Hugel, T.; Holland, N. B.; Cattani, A.; Moroder, L.; Seitz, M.; Gaub, H. E. Single-Molecule Optomechanical Cycle. *Science* **2002**, *296*, 1103−1106.
(14) Cembran, A.; Bernardi, F.; Garvelli, M.; Gagliardi, L.; Orlandi, G. On the Mechanism of the cis−trans Isomerization in the Lowest Electronic States of Azobenzene: S_0, S_1, and T_1. *J. Am. Chem. Soc.* **2004**, *126*, 3234−3243.
(15) Lednev, I. K.; Ye, T. Q.; Hester, R. E.; Moore, J. N. Femtosecond Time-Resolved UV−Visible Absorption Spectroscopy of trans-Azobenzene in Solution. *J. Phys. Chem.* **1996**, *100*, 13338−13341.
(16) Satzger, H.; Root, C.; Braun, M. Excited-State Dynamics of trans- and cis-Azobenzene after UV Excitation in the $\pi\pi^*$ Band. *J. Phys. Chem. A* **2004**, *108*, 6265−6271.
(17) Cusati, T.; Granucci, G.; Persico, M. Photodynamics and Time-Resolved Fluorescence of Azobenzene in Solution: A Mixed Quantum-Classical Simulation. *J. Am. Chem. Soc.* **2011**, *133*, 5109−5123.
(18) Bandara, H. M. D.; Friss, T. R.; Enriquez, M. M.; Isley, W.; Incarvito, C.; Frank, H. A.; Gascon, J.; Burdette, S. C. Proof for the Concerted Inversion Mechanism in the trans→cis Isomerization of Azobenzene Using Hydrogen Bonding to Induce Isomer Locking. *J. Org. Chem.* **2010**, *75*, 4817−4827.
(19) Fujino, T.; Arzhantsev, S. Yu.; Tahara, T. Femtosecond Time-Resolved Fluorescence Study of Photoisomerization of trans-Azobenzene. *J. Phys. Chem. A* **2001**, *105*, 8123−8129.
(20) Serra, F.; Terentjev, E. M. Effects of Solvent Viscosity and Polarity on the Isomerization of Azobenzene. *Macromolecules* **2008**, *41*, 981−986.
(21) Bandara, H. M. D.; Burdette, S. C. Photoisomerization in Different Classes of Azobenzene. *Chem. Soc. Rev.* **2012**, *41*, 1809−1825.
(22) Brown, C. J. A Refinement of the Crystal Structure of Azobenzene. *Acta Crystallogr.* **1966**, *21*, 146−152.
(23) Crecca, C. R.; Roitberg, A. E. Theoretical Study of the Isomerization Mechanism of Azobenzene and Disubstituted Azobenzene Derivatives. *J. Phys. Chem. A* **2006**, *110*, 8188−8203.
(24) Mostad, A.; Romming, C. A Refinement of the Crystal Structure of cis-Azobenzene. *Acta Chem. Scand.* **1971**, *25*, 3561−3568.
(25) Gagliardi, L.; Orlandi, G.; Bernardi, F.; Cembran, A.; Garavelli, M. A Theoretical Study of the Lowest Electronic States of Azobenzene: The Role of Torsion Coordinate in the cis−trans Photoisomerization. *Theor. Chem. Acc.* **2004**, *111*, 363−372.
(26) Hamm, P.; Ohline, S. M.; Zinth, W. Vibrational Cooling after Ultrafast Photoisomerization of Azobenzene Measured by Femtosecond Infrared Spectroscopy. *J. Chem. Phys.* **1997**, *106*, 519−529.
(27) Lednev, I. K.; Ye, T. Q.; Matousek, P.; Towrie, M.; Foggi, P.; Neuwahl, F. V. R.; Umapathy, S.; Hester, R. E.; Moore, J. N. Femtosecond Time-resolved UV-visible Absorption Spectroscopy of Trans-azobenzene: Dependence on Excitation Wavelength. *Chem. Phys. Lett.* **1998**, *290*, 68−74.
(28) Liang, Z.; Hai, M.; Wang, P.; Zhang, J.; Xie, J.; Zhang, Q. Nonlinearly Optical−Optical Isomerization Cycle in Azobenzene Liquid Crystal Polymers. *J. Appl. Phys.* **2001**, *90*, 5866−5870.
(29) Loudwig, S.; Bayley, H. Photoisomerization of an Individual Azobenzene Molecule in Water: An On−Off Switch Triggered by Light at a Fixed Wavelength. *J. Am. Chem. Soc.* **2006**, *128*, 12404−12405.
(30) Magee, J. L.; Shand, W., Jr.; Eyring, H. Non-adiabatic Reactions. Rotation about the Double Bond. *J. Am. Chem. Soc.* **1941**, *63*, 677−688.
(31) Curtin, D. Y.; Grubbs, E. J.; McCarty, C. G. Uncatalyzedsyn-anti Isomerization of Imines, Oxime Ethers, and Haloimines. *J. Am. Chem. Soc.* **1966**, *88*, 2775−2786.
(32) Dokic, J.; Gothe, M.; Wirth, J.; Peters, M. V.; Schwarz, J.; Hecht, S.; Saalfrank, P. Quantum Chemical Investigation of Thermal Cis-to-Trans Isomerization of Azobenzene Derivatives: Substituent Effects, Solvent Effects, and Comparison to Experimental Data. *J. Phys. Chem. A* **2009**, *113*, 6763.
(33) Anderson, J. A.; Petterson, R.; Tegner, L. Flash Photolysis Experiments in the Vapour Phase at Elevated Temperatures I: Spectra of Azobenzene and the Kinetics of its Thermal cis-trans Isomerization. *J. Photochem.* **1982**, *20*, 17−32.
(34) Brown, E. V.; Granneman, G. R. Cis-trans Isomerism in the Pyridyl Analogs of Azobenzene. Kinetic and Molecular Orbital Analysis. *J. Am. Chem. Soc.* **1975**, *97*, 621−627.
(35) Jaffe, H. H. A Reëxamination of the Hammett Equation. *Chem. Rev.* **1953**, *53*, 191−261.
(36) Amoros, J. G.; Ferrer, A. S.; Massad, W. A.; Nonell, S.; Velasco, D. Kinetic Study of the Fast Thermal cis-to-trans Isomerisation of Para-, Ortho- and Polyhydroxyazobenzenes. *Phys. Chem. Chem. Phys.* **2010**, *12*, 13238−13242.
(37) Matazo, D. R.; Ando, R. A.; Borin, A. C.; Santos, P. S. Azo−HydrazoneTautomerism in Protonated Aminoazobenzenes: Resonance Raman Spectroscopy and Quantum-Chemical Calculations. *J. Phys. Chem. A* **2008**, *112*, 4437−4443.
(38) Yi, Y.; Fang, G.; Maclennan, J. E.; Clark, N. A.; Dahdah, J.; Furtak, T. E.; Kim, K.; Farrow, M. J.; Korblova, E.; Walba, D. M. Dynamics of Cis Isomers in Highly Sensitive Amino-azobenzene Monolayers: The Effect of Slow Relaxation on Photo-induced Anisotropy. *J. Appl. Phys.* **2011**, *109*, 103521−5.
(39) Coelho, P. J.; Castro, M. C. R.; Raposo, M. M. M. Reversible trans−cis Photoisomerization of New Pyrrolidene Heterocyclic Imines. *J. Photochem. Photobiol., A* **2013**, *259*, 59−65.
(40) Hirose, Y.; Yui, H.; Sawada, T. Effect of Potential Energy Gap between the n-π^* and the π-π^* State on Ultrafast Photoisomerization Dynamics of an Azobenzene Derivative. *J. Phys. Chem. A* **2002**, *106*, 3067−3071.
(41) Gille, K.; Knoll, H. Quitzsch, Rate Constants of the Thermal cis-trans Isomerization of Azobenzene Dyes in Solvents, Acetone/Water Mixtures, and in Microheterogeneous Surfactant Solutions. K. *Int. J. Chem. Kinet.* **1999**, *31*, 337−350.
(42) Wildes, P. D.; Pacifici, J. G.; Iric, G.; Whitten, D. G. Solvent and Substituent Effects on the Thermal Isomerization of Substituted Azobenzenes. Flash Spectroscopic Study. *J. Am. Chem. Soc.* **1971**, *93*, 2004−2008.
(43) Wang, L.; Xie, J.; Zhou, H.; Yi, C.; Xu, W. Cis−trans Isomerization Mechanism of 4-Aminoazobenzene in the S_0 and S_1 States: A CASSCF and DFT Study. *J. Photochem. Photobiol., A* **2009**, *205*, 104−108.
(44) Wazzan, N. A.; Richardson, P. R.; Jones, A. C. Cis-Trans Isomerization of Azobenzenes Studied by Laser-Coupled NMR Spectroscopy and DFT Calculations. *Photochem. Photobiol. Sci.* **2010**, *9*, 968−974.
(45) Frisch, M. J.; Trucks, G. W.; Schlegel, H. B.; Scuseria, G. E.; Robb, M. A.; Cheeseman, J. R.; Montgomery, J. A., Jr.; Vreven, T.; Kudin, K. N.; Burant, J. C.; et al. *Gaussian 03*, revision B.05; Gaussian, Inc.: Pittsburgh, PA, 2003.
(46) Peng, C.; Schlegel, H. B. Combining Synchronous Transit and Quasi-Newton Methods to Find Transition States. *Isr. J. Chem.* **1993**, *33*, 449−454.
(47) Peng, C.; Ayala, P. Y.; Schlegel, H. B.; Frisch, M. J. Using Redundant Internal Coordinates to Optimize Equilibrium Geometries and Transition States. *J. Comput. Chem.* **1996**, *17*, 49−56.
(48) Miertus, S.; Scrocco, E.; Tomasi, J. Electrostatic Interaction of a Solute with a Continuum. A Direct Utilization of ab initio Molecular Potentials for the Prevision of Solvent Effects. *Chem. Phys.* **1981**, *55*, 117−129.
(49) Cossi, M.; Scalmani, G.; Rega, N.; Barone, V. New Developments in the Polarizable Continuum Model for Quantum Mechanical and Classical Calculations on Molecules in Solution. *J. Chem. Phys.* **2002**, *117*, 43−54.

(50) Reichardt, C. Solvatochromic Dyes as Solvent Polarity Indicators. *Chem. Rev.* **1994**, *94*, 2319−2358.
(51) Marcandalli, B.; Beltrame, P. L.; Pagila, E. D. Solvent and Viscosity Effect on the Kinetics of the Thermal cis-trans Isomerization of 3′-Nitro-4-Diethylaminoazobenzene. *Dyes Pigm.* **1989**, *11*, 179−189.
(52) Wang, L.; Wang, X. An ab initio Study of Stable Conformation and Thermal Isomerization of p-Amionazobenzene. *J. Mol. Stuct: THEOCHEM* **2007**, *806*, 179−186.
(53) Silva, D. L.; Krawczyk, P.; Bartkowiak, W.; Mendonca, C. R. Theoritical Study of One-and Two-photon Absorption Spectra of Azoaromatic Compounds. *J. Chem. Phys.* **2009**, *131*, 244516−244529.
(54) Kojima, M.; Nebashi, S.; Ogawa, K.; Kurita, N. Effect of Solvent on Cis-to-Trans Isomerization of 4-Hydroxyazobenzene Aggregated through Intermolecular Hydrogen Bonds. *J. Phys. Org. Chem.* **2005**, *18*, 994−1000.
(55) Kurita, N.; Nebashi, S.; Kojima, M. Density Functional Molecular Orbital Calculations on the Stability of Hydrogen-bonded 4-Hydroxyazobenzene Dimmers. *Chem. Phys. Lett.* **2005**, *408*, 197−204.
(56) *CRC Handbook of Chemistry and Physics*, 89th ed.; CRC Press: Taylor and Francis Group, 2008−2009; pp 6−197.